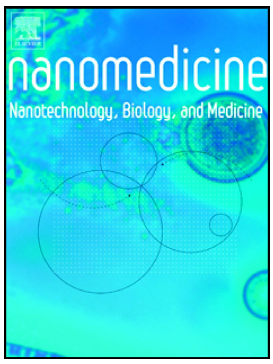

Discovery of nano-piperolactam a: A non-steroidal contraceptive lead acting through down-regulation of interleukins

Achintya Saha, Souvik Basak

PII: S1549-9634(18)30548-3
DOI: https://doi.org/10.1016/j.nano.2018.10.011
Reference: NANO 1895

To appear in: *Nanomedicine: Nanotechnology, Biology, and Medicine*

Revised date: 16 September 2018

Please cite this article as: Achintya Saha, Souvik Basak , Discovery of nano-piperolactam a: A non-steroidal contraceptive lead acting through down-regulation of interleukins. Nano (2018), https://doi.org/10.1016/j.nano.2018.10.011

Discovery of nano-piperolactam A: a non-steroidal contraceptive lead acting through down-regulation of interleukins

Plaban Bhattacharya[a], Achintya Saha[a], Souvik Basak[b*]

[a]Department of Chemical Technology, University of Calcutta, Kolkata 700009, India

[b]Dr. B.C. Roy College of Pharmacy and Allied Health Sciences, Durgapur 713206, WB, India.

*Author for correspondence: Souvik Basak
Ph: +91–9051226973
E-mail: souvik_basak1@yahoo.com

Authors' highest degree:
Plaban Bhattacharya: M. Pharm.
Achintya Saha: Ph.D.
Souvik Basak: Ph.D.

Word Count:

Abstract: 147 words

Total word count of the manuscript (including abstract, body of the text, figure legends, tables; excluding references): 5333

No. of Figures: 8

References: 60

No. of Tables: 2

Financial support

The study was initiated with the project received from University Potential of Excellence-Modern Biology (UPE-MB) scheme of UGC by Dr. A. Saha. Doctoral fellowship to Mr. P. Bhattacharya by the Council of Scientific and Industrial Research (CSIR, New Delhi) is thankfully acknowledged (09/028 (0814)/2010-EMR-I). The authors express no conflict of interest.

Conflict of Interest

The authors have declared that there is no conflict of interest.

Abstract

Elevated serum interleukins (IL-6, IL-1β) over baseline concentration help in blastocyst adhesion to the uterine endometrium in the early phase of pregnancy. A nano PLA (Piperolactam A)-HPBCD (2-hydroxy-propyl-β-cyclodextrin) inclusion complex, was developed as an interleukin down-regulator that exhibited 100% anti-implantation activity in rodents at a dose as low as 2.5–5.0 mg/kg. On metabolomics study, amongst major glyco-lipo-protein metabolites, only serum low-density lipoprotein (LDL) or very low-density lipoprotein (VLDL) levels revealed alteration by the formulation. Administration of PLA-HPBCD did not cause changes in serum estrogen and progesterone levels. However, IL-6 and IL-1β failed to increase post PLA-HPBCD administration, hence is assumed to be the mode of the drug's abortifacient action. In addition, absence of signs of either acute or chronic toxicity suggests the formulation considerably non-toxic. Therefore, the nano-PLA conjugate promises as a non-steroidal contraceptive lead apart from ormeloxifene, the only non-steroidal anti-fertility agent currently available globally.

Keywords: Piperolactam A, contraception, estrogen, progesterone, interleukin

Background

The frequent and unsupervised use of contraceptives causes numerous side effects, including increased blood transaminase and cholesterol levels, hypermenorrhea and intermenorrheal bleeding, indigestion, weight gain, and depression.[1] Searching new potent drugs that are less toxic, self-administrable, and less expensive is a challenging pursuit in the realm of pharmaceutical and medical sciences.[2] Plant drugs are generally considered as therapeutically safe and inexpensive, and the interest in the pharmacological role of plant-based bioactive compounds has increased in the last few decades.[3] Thus, antifertility agents

obtained from medicinal plants would provide immense benefits especially to inhabitants of developing countries, where the cost and safety profiles of these agents would be of keen interest.[4]

Piper betel Linn. (Piperaceae) is a perennial dioecious creeper, cultivated in India for its leaves since ancient times.[5] The leaves possess a wide range of pharmacological effects, such as antimicrobial, wound healing, cardiovascular, anti-inflammatory, immunomodulatory, antidiabetic, antiulcer, antipyretic, hepatoprotective, and neuroprotective potencies.[6,7] Harvested leaves are the economical products, and betel vine cultivation offers employment to millions of people.[8] The *Piper betel*Linn. root (PBR) is claimed to have ethnomedicinal use as a female contraceptive agent.[9,10] PBR contains a large number of bioactive molecules, such as diosgenin,[11] ursolic acid,[12] β-sitosterol, and other phytoconstituents.[12] The stalks and petioles of *P. betel* have anti-implantation effects.[14–17] Thus, *P. betel* can be effectively used as a source for discovering a novel antifertility drug.

Compared with natural cyclodextrins, the 2-hydroxypropyl derivative of β-cyclodextrin (HPBCD) has better complexation ability.[18,19] The application of HPBCD in oral drug delivery systems is acknowledged in various pharmacopoeias and national formularies.[20] It is noteworthy to mention that HPBCD has better aqueous solubility (thus better absorption in biological fluid) than β-cyclodextrin due to hydroxypropylation of certain hydroxyl groups within its structure which renders to reduce the strong crystallinity of the later and shifts the morphology to amorphous state.[21] Moreover, the hydrophobic core of HPBCD allows hydrophobic guest molecules to entrap within it (host)[22] which latter slowly releases the drugs upon aqueous solubilization. Since most of the compounds of *Piper betel* are hydrophobic in nature, we chose HPBCD as a promising candidate for future complexation with the extract or any isolated phytoconstituent.

Contraceptive drugs exhibit an antiestrogenic property by decreasing the secretion of gonadotropic hormones such as luteinizing hormone (LH) and follicle-stimulating hormone (FSH), eventually leading to blocking of ovulation.[23] In addition, the drugs may interfere with ovum and endometrium development, while others may have abortifacient or antiprogestational effects.[24–26] However, their indiscriminate use often leads to vigorous systemic illness or even fatal outcomes.[27-28] Therefore, it is necessary to study the toxicological and pharmacological actions of investigated drugs simultaneously for systemic standardization of the same. Metabolomics studies have demonstrated their enormous potential in elucidating toxicological mechanisms,[29–32] disease processes, and drug discovery.[33–35] The dynamic modeling of homeostatic processes could be achieved by monitoring the changes in the metabolic profiles of related biofluids and biomarkers.[36–38] Currently one drug available in the market namely ormeloxifene (centchroman)[39] which acts *via* non-steroidal pathway however with several side effects, thus potential non-steroidal contraceptive lead is always under search.

In course, we used the aforementioned contraceptive potential of *P. betel* Linn. to search the responsible biomolecule as a new therapeutic lead. First, in post extraction (or fractionation) phase, a PBR-HPBCD complex was fabricated to identify, study and perform biological investigations related to contraception. The PBR fraction was further characterized by relevant endocrinological, toxicological and serum metabolomics studies. We have used metabolite profiles of various biomarkers such as serum lipoproteins (such as LDL, VLDL), amino acids, glucose, glycoproteins, creatinine, pyruvic acid, lactic acid, choline, glycoproteins, serum albumins and such others to model the essential biochemical changes that have been brought in by the complex under investigation. Being the crucial analysis in drug discovery, acute and chronic toxicity studies were performed to determine either by visceral introspections or by molecular profiling of related biomarkers.

After confirmation, chromatography-based compound isolation was performed from the PBR extract. Post characterization, the compound was complexed with HPBCD to form a nano compound-HPBCD complex whose binding chemistry was examined through molecular docking studies. After re-confirming the abortifacient potential of the compound-HPBCD nano-complex, serum endocrinological profiling was performed for relevant gonadal and gonadotrophic hormones. Finally, the serum interleukin profile was investigated to understand the mechanism of action of the PLA-HPBCD complex.

Methods

Extract preparation

PBR was extracted by the hot percolation method in a Soxhlet extractor with 70% ethanol for 6 h. The hydrophobic molecules were discarded with *n*-hexane fractionation and the remaining residue after lyophilization was taken for further analysis.

Animal selection

Both male and female Wistar rats (200-250g) were used for the study. For any pharmacological or biochemical study, a group of six female rats (n= 6) were used. The Organisation for Economic Co-operation and Development (OECD) guidelines were followed for acute toxicity (guideline 420) and chronic toxicity (guideline 452) studies. For mating of animals, separate clean cages were used with male: female 2:1 ratio. During the course of the study, all the animals were maintained at 22±2 ºC, and supplied with standard food pellet and water *ad libitum*. All animal experiments performed in this study were approved by an Institutional Animal Ethics Committee (Reg. No.: 506/01/a/CPCSEA).

Detection of toxic metal elements, acute toxicity studies, and median lethal dose assessment

Toxic metals were detected using Atomic Absorption Spectroscopy by incinerating the extract for 30 min, followed by extraction with a nitric acid and hydrochloric acid mixture (3:1). For acute toxicity studies, mortality after 24 h was taken as the parameter of toxicity.

Nanoformulation development with PBR extract

The inclusion complex of PBR-HPBCD (1:1, w/w) formulation was prepared by co-evaporation technique.[40–43] PBR in 70% ethanol was mixed with 20 mM HPBCD solution in water and continuously stirred over a magnetic stirrer for 12 h. The resulting mixture was dried in a rotary evaporator with continuous shaking and stored after lyophilization for future studies. Particle size analysis was performed by dynamic light scattering (DLS) with hydrodynamic particle size and distribution assessments using a Zetasizer 2000 (Malvern Instruments, Malvern, UK). Particle morphology was assessed by scanning electron microscopy (Hitachi VP SEM, 3400N, Tokyo, Japan).

Dose selection for PBR-HPBCD complex

For post-coital contraceptive profile screening, four dose levels (125, 250, 400, and 500 mg/kg/day which are denoted as T1, T2, T3 and T4 respectively in this study) of the PBR-HPBCD complex were selected. The complex was orally administered in post-coital female Wistar rats from days 1–7 of pregnancy.

Evaluation of post-coital pregnancy interceptive activity

The pharmacological assessment of the contraceptive profile was performed as described earlier.[44-45] Briefly, adult female rats were subjected to intercourse with male rats in 2:1 ratio. The animals were laparotomized on the 16th day of pregnancy and uterine horns were diagnosed for the number and status of implants.

Determination of estrogenic/antiestrogenic activity

Estrogenic or antiprogesteronic activities were ascertained in adult female ovariectomized rats by measuring the dry weight of uterine horns after seven days of administration of control and test doses (the best dose obtained from a previous study) of the formulation. A 10% (v/v) solution of estradiol valerate at 1 mg/kg was used as synthetic estrogen.

Determination of progestational/antiprogestational activity

Progestational/antiprogestational activity was determined by dividing the immature female animals into four groups. Group I served as control, while the animals of groups II and IV were primed with progesterone (2 mg/kg subcutaneously daily), given for three days before traumatization. The traumatization was achieved by scratching the antimesometrial luminal lining of either horns using sterilized needles, with the other horn being a positive control. Group III was administered with test dose T2 while a combined dose of progesterone with T2 was administered to animals in group IV. The dosing schedule was continued for five days. After 24 h of the last dosing, animals were sacrificed by cervical dislocation. The weight of the uterine horns was measured after drying with a blotting paper.

Determination of variations in estrous cycles and serum gonadal and gonadotrophic hormones

Variations in estrous cycles were calibrated using both control (fed on solitary HPBCD in water for 21 days) and test (fed on 250 mg/kg/day PBR-HPBCD for 21 days) animals with respect to serum gonadal (estradiol and progesterone) and gonadotrophic (FSH and LH) hormones. Blood was collected from the retro-orbital plexus and serum was isolated after centrifugation and subsequent protein precipitation. ELISA with antihormonal antibodies was

performed for the quantitative screening of sera for elucidating the hormonal bias under investigation.

Pharmacometabolomics profiling

The animals were fed with the same dose of PBR-HPBCD formulation (250 mg/kg body weight), and metabolomics study was performed with blood collected from the retro-orbital plexus. 350 µL D_2O and 10 µL disodium-2,2-dimethyl-2-silapentane-5-sulfonate (DSS) solution (0.1% w/v) were added to 200 µL serum for NMR (Nuclear Magnetic Resonance) spectroscopy analysis (600.44 MHz, Bruker, USA). Any interference by water was suppressed by excitation sculpting. Spectrums were processed by MNova v.8.1.0 software. Each spectrum was calibrated with respect to the DSS peak area, and properly phased, baseline corrected, and aligned peaks were integrated into bins across the spectral regions of 0.04 ppm. The assignment of the spectral peaks to specific metabolites was achieved, mean-centered and pareto-scaled ($1/\sqrt{SD}$) data were transposed and analysis was performed in STATISTICA. PCA (Principle Component Analysis) and PLS-DA (Partial Least Square Discriminant Analyses) were performed in the dataset compared to the control group.[44]

Test of reversibility of antifertility effect and chronic toxicity studies

Normal behavioral parameters, such as food intake, body weight gain, and stool quality, were monitored for adult female rats for one month. Competent rats (n=24) with normal physiological cycles were divided into two groups (n=12), subjected to PBR-HPBCD or solitary polymer dosing for 21 days, and left untreated for another 21 days. Two sub-groups (n=6) were created for each above group of rats. The first subgroup was subjected to mating with males at the pro-estrous phase. After one gestation cycle, the number of litters, average weight of pups on day 7 and viability index were checked.

Blood was collected from the other subgroup of animals followed by sacrifice, and histopathological analyses were performed with liver, kidney, and lung samples. Serum biomarkers such as SGPT (Serum Glutamic Pyruvic Transaminase) and SGOT (Serum Glutamic Oxaloactatic Transaminase), ALP (Alkaline Phosphatase), creatinine and uric acid, MDA (Malondialdehyde), GSH (Reduced Glutathione), and NO (Nitric Oxide) were also evaluated as reported earlier.[45]

Bioactivity-guided fractionation, compound isolation, and nanocomplexation with HPBCD

Bioactivity-guided fractionation, compound isolation, HPBCD complex formation, and characterization studies were performed as described earlier.[43] Briefly, the compound was isolated from the *n*-hexane:ethyl acetate (50:50) fraction of the ethyl acetate extract of *P. betel*. The said fraction was subjected to preparative thin layer chromatography with toluene-ethyl acetate-methanol (3:2:1) as the mobile phase, and the most intense band under 366 nm was cut off. The bound compound was dissolved in methanol, dried, and subjected to spectroscopic analysis (FT-IR, NMR, MS) for characterization. The isolated compound, Piperolactam A (PLA) was subsequently complexed with HPBCD as reported earlier to form PLA-HPBCD complex.[43]

Molecular dynamics simulation-ligand-receptor binding

Molecular dynamics (MD) was performed to study the interaction between the receptor and ligand in an active condition. Therefore, in the present study, MD analysis was performed after docking the ligand, PLA, with human progesterone (PDB ID: 1E3K) and estrogen receptors (PDB: 1ERE). MD simulation was undertaken in a TIP3P water model (i.e., transferable intermolecular potential 3P) in Desmond/Maestro using the OPLS (Orthogonal Partial Least Square) molecular mechanics force field. Nose-Hoover chain thermostat and

Martyna-Tobias-Klein barostat were captured at 300 K and at 1.013 bar pressure for the equilibration of temperature and pressure.

In vitro release profile

In vitro release profile of PLA from PLA-HPBCD was performed as described earlier[43], with a control of unformulated solitary PLA subjected to release under the same condition for evaluating both individual and comparative release kinetics between the two.

Statistical analysis

Kinet DS software[46] and Microsoft Excel (Microsoft Corporation, USA) were used to model the release profile of PLA from the formulation. The percentage dissolution efficiency (% DE)[47-48], mean dissolution time (MDT)[49], difference (f_1) and similarity (f_2) factor[50] were determined as per the standard protocol.

LD_{50} of PLA-HPBCD complex

For the acute toxicity study, PLA-HPBCD was administered orally at single doses of 0.1, 0.2, 0.5, 1, 1.5, and 2 g/kg body weight to individual groups (n=6, each). Mortality after 24 h was considered as the parameter of toxicity.

Contraceptive property assessment

The contraceptive potential of PLA-HPBCD was assessed as described above for PBR-HPBCD. However, the chosen doses of the PLA-HPBCD were 2.5, 5, and 10 mg/kg body weight.

Evaluation of hormonal profile alteration

Alteration in the hormonal profile was assessed after administering PLA-HPBCD (5.0 mg/kg), with respect to normal pregnant group. Blood was withdrawn from the retro-orbital plexus on 7th post-coital day after mating, and the hormonal profile in serum was assayed using ELISA.

Serum interleukin assay

Blood was collected from the retro-orbital plexus of female rats under treatment on PLA-HPBCD, 5.0 mg/kg body weight, before and on 7th post-coital day of mating, and serum interleukin concentration was determined using a standard anti-mouse anti-interleukin antibody by a 96-well bioplate assay.[51]

Results

Arsenic, cadmium, and lead contents in the PBR extract were in compliance with the allowed limits (<5 ppb), mentioned in US-FDA and AYUSH guidelines.[52-53] Animals administered with ≤3.5 g/kg of PBR extract showed reduced mobility (hypoactivity); however, other signs of toxicity were not observed at doses ≤3.5 g/kg. With increased dose, dose dependent mortality was observed. The oral LD_{50} of PBR was found to be 5.00 g/kg (Supplementary Figure S1). After PBR extract was chelated with HPBCD, the mean particle size of the PBR-HPBCD formulation was 585.0 nm and the polydispersity index was 0.288 (DLS, Figure 1A). Spherical rough particles were observed through Scanning Electron Microscopy (SEM) analysis (Figure 1B). Moreover, these particles were found stable even after one month which was deduced from the SEM analysis of the nano PBR-HPBCD complex after one month of their preparation. The post-month SEM image (Supplementary Figure S2) revealed that the complex particle diameter having no appreciable decay of surface morphology or size (~ 500 nm).

PBR-HPBCD demonstrated anti-implantation potential in an oral dose-dependent manner (Figure 2A). Moreover, PBR-HPBCD at a dose of ≥250 mg/kg did not show conception (Figure 2B), however caused behavioral changes (reduced locomotion or hypoactivity) at a dose of 500 mg/kg (T4). Thus, PBR-HPBCD at a dose of 250 mg/kg (T2) was revealed as the minimum effective dose to cause 100% pregnancy interception (n=20); therefore, this dose was considered for subsequent pharmacological studies (Table 1).

In ovariectomized rats, PBR-HPBCD (T2) exerted a negligible estrogenic action. The uterine weight was slightly enhanced. However, the action of estrogen was inhibited significantly when T2 was administered with estradiol valerate (EV) (Figure 3A). T2 did not have any progestational activity; neither agonistic nor antagonistic (Figure 3B). The detailed data of estrogenic/antiestrogenic and progesteronic/antiprogesteronic activities are reported in Supplementary Tables S1 and S2.

In serum metabolomics investigation, as a classifier, the score plots were checked for clustering trends and outliers. Figure 4A depicts the NMR spectra of serum of normal rats' cycle in the proestrus phase. Till date, this is the first report to describe the serum metabolite content of female rats in the proestrus phase, obtained by NMR spectroscopy after using selective 180° pulses for water suppression. The spectrums obtained from the serum of treated groups of the ethnomedicinal formulation (PBR extract) and the developed formulation (PBR-HPBCD) are shown in Figure 4B and 4C, respectively. Visual screening could not detect the subtle metabolite changes. After orthogonal signal correction, PLS analysis was performed and a significant difference between pre- and post-treatment period was observed (Figure 5A and 5B). The differences among groups were correlated with first (R^2 = 0.434) and second (R^2 = 0.251) components. Ethnomedicinal formulation of PBR elevated LDL and VLDL cholesterol levels (Figure 5C and 5D). Relative quantification over the selective shift regions (δ of 0.85 and 1.26) exhibited adequate separation ($p<0.005$). 0.85

and 1.26 shifted protons are of Low density lipoprotein (LDL) and Very Low density Lipoprotein (VLDL) peaks. δ 0.85 indicated terminal $–CH_3$ groups which are under least electromagnetic shielding whereas δ 1.26 are methylenic ($-CH_2$) protons that are close to the cholesterol ring . Considerable separation (height and area) of these two proton peaks between untreated and treated groups of PBR-ethanolic extract suggests that in PBR-treated group LDL/VLDL level varies notably (Figure 4A, 4B and 5C, 5D). However, for other metabolites, the scores of pre- and post-treated samples were not well separated in the PBR-HPBCD-treated group (Figure 5A and 5B). Statistically non-significant metabolite fluctuations were detected (Figure 5E and 5F).

An ideal contraceptive agent should possess the ability to revert the antifertility activity on withdrawal, which was evaluated in our study by chronic toxicity estimation of T2. After contraceptive withdrawal, a significant number of litters were born with 100% viability, suggesting the reversible nature of the contraceptive (Table 2). Morphological and histopathological investigations did not show any signs of organ damage in test animals compared with control animals (Supplementary Figure S3). The liver marker enzymes, Serum Glutamic Pyruvic Transaminase (SGPT), Serum Glutamic Oxaloacetic Transaminase (SGOT), and Alkaline Phosphatase (ALP), varied only 7.04%, 0.56%, and –2.76%, respectively, compared with their normal baseline levels (Table 2). Renal functional parameters, lipid peroxidation markers, and antioxidant profile did not reveal considerable variation in test animals compared with control animals.

Uterine horns were observed under microscope (Supplementary Figure S4) for post coital pregnancy interceptivestudy of PBR-HPBCD at a dose of 250 mg/kg (T2). Without the test dose, clear bulb like swollen uterine horns were visible (Supplementary Figure S4A) on 16^{th} day of pregnancy, which suggests conception of the embryo within the uterine horn. However on administration of T2, after same days of coitus, thin tube like uterus was

observed without any prominent sac like horn suggesting absence of conception (Suplementary Figure S4B). Corpora lutea were visible on both uterus without (Supplementary Figure S3C) or with (Supplementary Figure S3D) test dose, however, the number of the lutea were revealed lesser in T2 fed uterus than that that of control (Table 1).

Bioactivity-guided fractionation and the subsequent response of the PBR extract as an anti-fertility agent helped us to isolate PLA, the main constituent of the PBR extract.[43] The size of the complex was 180 nm.[43] Moreover, the nanoparticles were nearly spherical (Figure 6). The binding interactions, as well as the inclusion of the drug inside the HPBCD cavity, were investigated by Fourier Transform Infrared FT-IR spectroscopy and drug-polymer docking studies, which are discussed later.

The baseline evaluation of the value-added nano-drug conjugate was done by testing the conjugate's bioavailability improvement through *in vitro* release. When the conjugate was released from the polymer matrix, its release profile was >8 times (94.66% release) more of the release profile of the crude drug (11.33% release, Figure 6D). A low similarity factor (f_2) of 10.10 and a high difference factor (f_1) of 841.86 between the drug release profiles showed that nanofabrication of PLA significantly altered the solubility profile of the crude drug. Model-independent analyses were used and zero-order release (Supplementary Figure S5A) showed the best regression (R^2 = 0.7506), indicating a steady prolong release of the drug from the formulation. Furthermore, total release of the drugs followed symmetry with Weibull model with lag time (R^2 = 0.9997) (Supplementary Figure S5B).

Although PLA-HPBCD complex formation was undertaken and reported in our previous study, the docking studies conducted here revealed the binding mechanism of PLA inside HPBCD. Interestingly, the docking interaction revealed inclusion of the phenanthrene nucleus within the HPBCD central cavity (Figure 7A). *In silico* bonding interactions revealed that the -NH hydrogen undergoes hydrogen bonding with two adjacent glucopyranose

hydroxyl groups (Figure 7A, 7B). In addition, the lactam carbonyl oxygen in equilibrium with its tautomeric form rendered hydrogen bonding with hydroxyl functionalities of two neighboring carbohydrate rings (Figure 7B).

During acute toxicity studies, a single dose of PLA-HPBCD at <0.5 g/kg exhibited reduced physical mobility (hypoactivity), but significant toxicity (such as changes in fur and skin colour, respiratory depression, increase of body temperature, impairment of somatomotor activity, convulsion, cardiac depression, salivation, diarrhoea, changes in eye colour as per OECD guidelines as mentioned earlier) was not observed in the animals. At higher doses, a regular dose-dependent rise in mortality was observed. The oral LD_{50} of PLA has been estimated as 787 mg/kg (Supplementary Figure S6A) while that of PLA-HPBCD was ~ 1.00 g/kg (Supplementary Figure S6B). In a cell line evaluation, a cytotoxicity index at 900 µM against mouse peritoneal macrophage cells suggested a fair safe therapeutic profile of PLA-HPBCD.[43]

PBR-HPBCD complex stopped conception at 250 mg/kg, contraception was 100%; while the PLA-HPBCD complex at the dose level of 2.5 mg/kg revealed 1 litter born out of 8.3 litters (n=6), conception and contraception has been 12.05% and 87.95% (Table 1). At 5.0 mg/kg of PLA-HPBCD, no sign of fertilization was visible in rats. A further serum endocrinological analysis revealed that serum estradiol and progesterone levels were not much altered between control and PLA-HPBCD treated groups. The estradiol levels in control and treated groups were found to be 86.74 ±1.65 and 84.16 ±2.05 pg/mL, respectively. Whereas progesterone level was found 115.24 ±2.16 and 109.54 ±1.72 ng/mL (n=6), reveals no significant alteration in hormonal profile with respect to control (Figure 8A). The serum interleukin assay revealed that serum IL-1β and IL-6 concentrations remained almost unaltered in between post-coital day 1 and 7 (Figure 8B). The IL-1β concentration was found to be 17.01 ± 0.80 and 17.69 ± 0.97 pg/mL before mating and on 7th

day after mating respectively ($p > 0.05$). Again, IL-6 concentration showed a negligible increase after parturition (31.69 ± 0.99 pg/mL from 29.69 ± 0.91 pg/mL before mating and on 7th day after mating respectively).

Discussion

Except some reduced locomotor activity which may be due to reduction of nor-adrenergic transmission in animal body according to earlier reports,[54] the PBR extract showed considerably low toxicity profile in rats. The PBR-HPBCD complex having PLA as a major phytoconstituent has been revealed to possess safe metabolite dynamics in physiological fluids. From our metabolomic data and score plot, it may be proposed that the incorporation of cyclodextrin with the extract preparation probably has a beneficial effect on low-density lipid profiles. The bioavailability of hypolipidemic terpenoids might be enhanced. From the score plot, we could suggest that cyclodextrin complexation facilitated a better elimination rate of xenobiotics.

The isolation of PLA and eventual incorporation within HPBCD with a 100–200-nm nanoinclusion complex followed release mimicking Weibull model with lag time,[46-47]*in vitro*. The models analyzed suggest that the formulated PLA nanoparticles are spherical with sufficient porosity to allow the drug to slowly diffuse across the polymer matrix.[48–50] Furthermore, the % DE of the nanoformulated PLA (72.45%) was about nine times more than the%DE of the non-formulated PLA (8.24%), while the MDT of the nanoformulated PLA was much lower (71.21) compared with the MDT of the crude drug (81.72) suggesting a significant improvement of drug release in the nano condition than in the crude form. The improvement of PLA solubility could further improve its bioavailability by augmented passive diffusion of the same from concentrated gastrointestinal fluid to all biological matrix (without considering active transport at this investigational stage). The possible improvement

of bioavailability can also be suggested by nanonization of the drug which follows a complicated relationship with lipid membrane permeability. Briefly, it can be concluded that reducing particle diameter (z) increases the size dependent surface energy (γsv) of the nano-system (Equation 1, Section 2, Supplementary Information) and increasing surface energy (γsv) increases Diffusion coefficient D (z) assuming resistance of the lipid membrane S (z) is constant for a particular case (Equation 2, Section 2, Supplementary Information). Increment of Diffusion coefficient subsequently increases lipid membrane permeability of the nano-system.

The PLA-HPBCD docking analysis performed in this study showed incorporation as well as hydrogen bonding as the major holding interaction of the formulation. This concurs with our previous observations of FT-IR spectra, where characteristic phenanthrene vibration at 1452 cm^{-1}(aromatic –C=C- stretch) was suppressed after complex formation with HPBCD (Supplementary Figure S7).[43] Experimentally, the peak of PLA at 1616 cm^{-1} was shifted to 1610 cm^{-1} probably because of the hydrogen bond formation involving the secondary amine (-NH-)[42] (Supplementary Figure S7). Furthermore, the carbonyl oxygen in equilibrium with its tautomeric form rendered hydrogen bonding with hydroxyl functionalities of two neighboring carbohydrate rings (Figure 7B). The bonding interaction was again supported by IR positional shift[42] where the carbonyl stretching at 1656 cm^{-1} was shifted to 1689 cm^{-1}.

The low toxicity of the candidate molecule is at par with our previous findings[55] that PLA could not induce significant inhibition of cardiac human ether-a-go-go related gene (hERG) receptors (that regulate potassium ion channel on heart muscle) , nuclear receptors, or liver cytochrome P450 proteins. Since the binding between PLA and corresponding gestogenic receptors was observed by molecular dynamic simulation in our earlier report,[55] we considered a realistic model using rodents in this study.

A dose-dependent analysis revealed that the minimum abortifacient dose of PBR-HPBCD was 250 mg/kg, while that of the nano PLA conjugate was 2.5–5.0 mg/kg. Thus, the potency improved about 100 times when PLA was administered in a nanoformulation with HPBCD. Therefore, we propose that nano PLA might penetrate biological membranes efficiently because of its smaller particle size, higher surface energy, and HPBCD-guided P-glycoprotein inhibition at biological membranes.[56]

Serum gonadotropic (FSH and LH) and gonadal (estrogen and progesterone) endocrinological analyses showed that the chief reproductive hormones (estrogen and progesterone) did not increase even after mating after PLA-HPBCD administration at 5.0 mg/kg. The sustenance of the hormonal levels can be explained by the lower stimulation of FSH and LH (as described earlier), which is compensated again by displaced estradiol through low to moderate PLA-estrogen receptor binding.[55] However, it is not clear why the PBR extract lowered the serum hormonal profile but PLA did not. Probably the steroidal constituents of the PBR extract, such as diosgenin, ursolic acid, and β-sitosterol,[11-13] interfered strongly with the steroidal pathway *in vivo*; these constituents are absent in PLA, which is basically an aristolactam alkaloid.

To reveal the possible mechanism of contraception, we estimated the serum interleukin concentration using ELISA with a standard anti-mouse anti-interleukin antibody. Because previous studies have reported that the increase in serum interleukin concentration is required for blastocyst adhesion to the uterine endometrial lining in the early phase of pregnancy,[67–68] In our study also, in control pregnant group IL-1β and IL-6 concentrations raised to 21.04 ± 1.21 pg/mL and 35.52 ± 0.98 pg/mL respectively from 17.01 ± 0.80 pg/mL and 29.69 ± 0.91 pg/mL respectively.

it is pertinent to evaluate serum interleukins to investigate the possible pathway of contraception. IL-6 and IL-1β were kept at baseline level in post-coital rats after PLA-

HPBCD administration (serum analyzed after seven days of mating). This may have de-activated integrin expression in the blastocyst[59] (integrin is a protein upregulated in blastocysts during the early phase of pregnancy and is required for blastocyst adhesion to the uterine endometrial lining), subsequently leading to contraception.

We further investigated if there was any rational or direct involvement of PLA in downregulating IL-6 and IL-1β. An across-the-board study revealed that interleukin biosynthesis is a complicated intertwined network that involves several proteins and transcription factors such as Protein Kinase C, cAMP responsive element, nuclear factor-κB (NF-κB), activator protein-1, and CCAAT/enhancer binding protein.[59] PLA has been acknowledged to inhibit NF-κB and subsequently block interleukin expression,[60] which concurs with the results of serum interleukin output after nano PLA administration in the present study. Our study suggested that PLA-HPBCD guided deactivation of IL synthesis prevented the additional increment of IL-6 and IL-1β in pregnant rats serum (Figure 8) thus forcing them to refrain from their conception mechanism. This in turn, provoked the abortifacient mechanism of PLA-HPBCD nano conjugate. However, the retention of IL concentration at near basal level could possibly retain the other pathophysiological roles of IL in blood. Till date only ormeloxifene is available in market as a considerably safe non-steroidal contraceptive (0.25 mg/kg for five consecutive days post coitus on rats).[39] We suggest that, the PLA-HPBCD nanoconjugate has the potential to evolve as an alternate non-steroidal contraceptive lead worldwide with further clinical studies.

References

1. Unny R, Chauhan AK, Joshi YC, Dobhal MP, Gupta RS. A review on potentiality of medicinal plants as the source of new contraceptive principles *Phytomedicine* 2003;**10**: 233–260.
2. Ulrich-Merzenicha G, Panekb D, Zeitlerb H, Wagnerc H, Vetter H.New perspectives for synergy research with the "omic"-technologies.*Phytomedicine* 2009;**16**: 495-508.
3. Goonasekera MM, Gunawardana VK, Jayasena K, Mohammed SG, Balasubramaniam S.Pregnancy terminating effect of *Jatrophacurcas* in rats. *J Ethnopharmacol*1995,**47**: 117–23.
4. Brinker F. Inhibition of endocrine function by botanical agents, Antigonadotrophic activity. *British J. Phytother* 1997; **4**: 123-145.
5. Ghosh K, Bhattacharya TK.Chemical constituents of *Piper betel* Linn. (Piperaceae) roots. *Molecules* 2005;**10**: 798-802.
6. Periyanayagam K, Jagadeesan M, Kavimani S,Vetriselvan T.Pharmacognostical and Phyto-physicochemical profile of the leaves of *Piper betel* L. *var*Pachaikodi (Piperaceae) - Valuable assessment of its quality. *Asian Pac J Trop Biomed* 2012;**2**: S506–S510.
7. Chandra V, Tripathi S, Verma NK,Singh DP, Chaudhary SK,Roshan A. Piper betel phytochemistry, traditional use and pharmacological activity-a review.*Int J Pharm Res Dev* 2012;**4**: 216-223.
8. Kumar N.Betel vine (*Piper betel*L.) cultivation: A unique case of plant establishment under anthropogenically regulated microclimatic conditions.*Indian J HistSci* 1999;**34**, 19–32.

9. Ranjan PM, Manujshree M, Sabita M, Samira S. Antifertility effect of alcoholic stalk extract of *Piper betel* Linn on female albino rats. International Research Journal of Pharmacy 2013; **4**: 218-220.
10. Sarkar M, Gangopadhyay P, Basak B, Chakrabarty K, Banerji J, Adhikary P, Chatterjee A.The reversible antifertility effect of *Piper betel* Linn. on Swiss albino male mice. *Contraception* 2000, **62**, 271-274.
11. Dixit BS, Banerji R, Johri JK, Bhatt GR, Sircar KP. Diosgenin, a constituent of *Piper betel*L. root. *Indian J Pharm Sci* 1995;**57**: 263-264.
12. Saeed SA, Farnaz S, Simjee RU, Malik A. Triterpenes and ß-sitosterol from Piper *betel*: Isolation, antiplatelet and anti-inflammatory effects. *BiochemSoc Trans* 1993; **21**: 462S.
13. Parmar VS, Jain SC, Gupta S, Talwar S, Rajwanshi VK, Kumar R et al. Polyphenols and alkaloids from *Piper species*. *Phytochemistry* 1998; **49**: 1069-1078.
14. Adhikary P, Banerji J, ChowdhuryD, Das AK, Deb CC, Mukherjee SR et al. Antifertility effect of *Piper betel* L. extract on ovary and testis of albino rats. *Indian J ExpBiol*1989; **27**: 868-870. http://pubget.com/paper/2635145.
15. Sharma JD, Sharma L, Yadav P. Antifertility efficacy of *Piper betel*Linn. (Petiole) on female albino rats. *Asian J Exp Sci* 2007; **21**: 145-150.
16. Pradhan MR, Mohanty M, Mohapatra S, Sahoo S. Antifertility effect of alcoholic stalk extract of Piper betel Linn. on female albino rats. *Int Res J Pharm* 2013; **4**: 218-220.
17. Loftsson T, Duchene D. Cyclodextrins and their pharmaceutical applications. *Int J Pharm* 2007; **329**: 1-11.

18. Al Omari AA, Al Omari MM, Badwan AA, Al-Souod KA. Effect of cyclodextrins on the solubility and stability of candesartan cilexetil in solution and solid state. *J Pharm Biomed Anal* 2011; **54**: 503-509.

19. Challa R, Ahuja A, Ali J, Khar RK. Cyclodextrins in drug delivery: An updated review. *AAPS Pharm Sci Tech* 2005; **6**: E329-E357

20. Gark SK, Mathur VS, Chaundhury RR. Screening of Indian Plants for anti-fertility activity. *Ind J Exp Biol* 1978; **16**:107–118

21. Chordiya Mayur A, Senthilkumaran K. Cyclodextrin In Drug Delivery: A Review Research and Reviews: *J Pharm Pharm Sci*. 2012; **1**: 19-29

22. Anonymous. HPBCD as anticancer drug. *Resume of PLoS ONE* **10**: e0141946

23. Yakubu MT, Bukoye BB. Abortifacient potentials of the aqueous extract of *Bambusa vulgaris* leaves in pregnant Dutch rabbits. *Contraception* **80**: 308–313, 2009.

24. Christin-Maitre S, Bouchard P, SpitzIM. Medical termination of pregnancy. *The New Eng J Med* 2000; **342**: 946–956.

25. Keshria G, Lakshmi V, Singh MM. Pregnancy interceptive activity of Meliaazedarach Linn. in adult female Sprague-Dawley rats. *Contraception*2003; **68**: 303–306.

26. Cigand C, Laborde A. Herbal Infusions Used for Induced Abortion. *J Toxicol: Clinical Toxicol* 2003; **41**: 235–239

27. Chao Ma, Kaishun Bi, Ming Zhang, Dan Su, Xinxin Fan, Wei Ji et al. Toxicology effects of Morning Glory Seed in rat: A metabonomic method for profiling of urine metabolic changes. *J Ethnopharmacol* 2010;**130**: 134-142

28. Li L, Suna B, Zhang Q, Fang J, Ma K, Li Y, et al. Metabonomic study on the toxicity of Hei-Shun-Pian, the processed lateral root of *Aconitum carmichaelii* Debx. (Ranunculaceae). *J Ethnopharmacol* **2008**; 116: 561-568

29. Dai Y, Li Z, Xue L, Dou C, Zhou Y, Zhang L. Metabolomics study on the anti-depression effect of xiaoyaosan on rat model of chronic unpredictable mild stress. *J Ethnopharmacol* 2010; **128**: 482-489

30. Liu NQ, Cao M, Frédérich M, Choi YH, Verpoorte R, van der Kooy F. Metabolomic investigation of the ethnopharmacological use of *Artemisia afra* with NMR spectroscopy and multivariate data analysis. *J Ethnopharmacol*2010; **128:** 230-235, 2010.

31. Raamsdonk LM, Teusink B, Broadhurst D, Zhang N, Hayes A, Walsh MC et al. A functional genomics strategy that uses metabolome data to reveal the phenotype of silent mutations. *Nature Biotechnol* 2001; **19**: 45–50

32. Oliver DJ, Nikolau B, Wurtele ES. Functional Genomics: High-Throughput mRNA, Protein, and Metabolite Analyses. *Metab Eng* 2002; **4**: 98–106.

33. Lindon JC, Nicholson JK, Holmes E, Antti H, Bollard ME, Keun H et al. Contemporary issues in toxicology the role of metabonomics in toxicology and its evaluation by the COMET project. *Toxicol Appl Pharmacol* 2003; **187**: 137–146.

34. Beckonert O, Bollard ME, Ebbels TMD, Keun HC, Antti H, Holmes E et al. NMR-based metabonomic toxicity classification: hierarchical cluster analysis and k-nearest-neighbour approaches. *Anal Chim Acta* 2003; **490**: 3–15

35. Griffin JL. The potential of metabonomics in drug safety and toxicology. *Drug Discov Today: Technol* 2004; 1: 285–293

36. Lenza EM, Bright J, Knight R, Wilson ID, Major H. Cyclosporin A-induced changes in endogenous metabolites in rat urine: a metabonomic investigation using high field Full-size image (1 H) NMR spectroscopy, HPLC-TOF/MS and chemometrics. *J Pharm Biomed Anal* 2004;**35**: 599–608

37. Garrod S, Bollard ME, Nicholls AW, Connor SC, Connelly J, Nicholson JK et al. Integrated Metabonomic Analysis of the Multiorgan Effects of Hydrazine Toxicity in the Rat. *Chem Res Toxicol* 2005;**18**: 115–122

38. Keun HC. Metabonomic modeling of drug toxicity. *Pharmacol Therapeutics* 2006; 109: 92–106

39. Kamboj VP, Ray S, Anand N. Centchroman: A safe reversible postcoital contraceptive with curative and prophylactic activity in many disorders. *Frontier Biosci* 2018; **10**:1-14

40. Pandya P, Gattani S, Jain P, Khirwal L, Surana S. Co-solvent evaporation method for enhancement of solubility and dissolution rate of poorly aqueous soluble drug simvastatin: *in-vitro* and *in-vivo* evaluation. *AAPS Pharm Sci Tech* 2008; **9**: 1247-1252.

41. Purkayastha P, Jaffer SS, Ghosh P. Physicochemical perspective of cyclodextrin nano and microaggregates. *Phys Chem Chem Phys* 2012; **14**: 5339-5348.

42. Bilensoy E, Gurkaynak O, Ertan M, Sen M, Hincal AT. Development of nonsurfactant cyclodextrin nanoparticles loaded with anticancer drug paclitaxel. *J Pharm Sci* 2008; **97**:1519-1529.

43. Bhattacharya, P, Mondal S, Basak S, Das P, Saha, A., Bera T. *In vitro* susceptibilities of wild and drug resistant *Leishmania donovany* amastigotes to Piperolactam A loaded hydroxypropyl β-cyclodextrin loaded nanoparticles. *Acta tropica* 2016; **158**, 97-106

44. Bhattacharya P, Saha S. Evaluation of reversible contraceptive potential of *Cordia dichotoma* leaves extract. *Brazilian J Pharmacognosy* 2013; **23**: 342-350

45. Dickerson J, Bressler R, Christian CD. Liver function tests and low dose oral contraceptives. *Contraception* 1980; **22**: 597-603

46. Mendyk A, Jachowicz R, Fijorek K, Dorożyński P, Kulinowski P, Sebastian P. KinetDS: an open source software for dissolution test data analysis. *J Disso Technol* 2012; **19**: 6-11

47. Khan KA. The concept of dissolution efficiency. *J Pharm Pharmaco*l 1975; **27**: 48-49.

48. Costa FO, Sousa JJS, Pais AACC, Formosinho SJ. Comparison of dissolution profiles of Ibuprofen pellets. *J Controlled Release* 2003; **89**: 199–212.

49. Costa P, Sousa Lobo JM. Modeling and comparison of dissolution profiles. *Eur J Pharm Sci* 2001; **13**: 123–133.

50. Shoaib MH, Siddiqi SAS, Yousuf RI, Zaheer K, Hanif M, Rehana S et al. Development and evaluation of hydrophilic colloid matrix of famotidine tablets. *AAPS Pharma Sci Tech 2010*; **11**:708-718

51. Hauser SP, Kajkenova O, Lipschitz DA. The Pivotal Role of Interleukin 6 in formation and function of Hematopoietically active murine long-term bone marrow cultures. *Stem Cells* 1997; 15: 125-132

52. https://www.fda.gov/Food/FoodborneIllnessContaminants/Metals/ucm280755.htm

53. Anonymous. General guidelines for drug development of Ayurvedic formulations. Central Council for Research in Ayurvedic Sciences 2018, First Edition.

54. Vyawahare NS, Bodhankar SL. Neuropharmacological profile of *Piper betel* leave extracts in mice. Pharmacologyonline 2007; **2**: 146-162

55. Amin SK, Bhattacharya P, Basak S, Gayen S, Nandi A, Saha A. Pharmacoinformatics study of Piperolactam A from *Piper betel* root as new lead for non-steroidal anti-fertility drug development. *Comput Biol Chem* 2017; **67:** 213-224

56. Zhang Y, Meng FC, Cui YL, Song YF. Enhancing effect of hydroxypropyl-ß-cyclodextrin on the intestinal absorption process of genipin. *J Agric Food Chem* 2011; **59:** 10919-10926.

57. BibaM, Keramitsoglou T, Goukos D, Verla-lefthireoti M, Pantos K, Koumantakis G, Makrigiannakis A, Messinis IE. Interleukin 1(IL)-1 beta and IL-6 levels in human embryo culture cells supernatants and their role in supernatants and their role in implanatation following IVF: a prospective non-randomised study. *J Immuno Biol* 2016; **1**:105

58. Moreli JB, Ruocco AC, Vernini JM, Rudge MVC, Calderon IMP. Interleukin 10 and tumor necrosis factor-Alpha in pregnancy: aspects of interest in clinical obstetrics. *ISRN Obstet Gynecol* 2012; doi:10.5402/2012/230742

59. Lu H, Wu JY, Kudo T, Ohno T, Graham DY, Yamaoka Y. Regulation of Interleukin-6 promoter activation in gastric epithelial cells infected with *Helicobacter pylori*. *Molecular Biology of the Cell* 2005; **16**: 4954-4966

60. Wiart C. Lead Compounds from Medicinal Plants for the Treatment of Neurodegenerative Diseases. *Science Direct* 2014; ISBN: 978-0-12-398373-2

Figure legends:

Figure 1. Characterization of PBR-HPBCD complex (A) DLS (B) SEM

Figure 2. Assessment of the contraceptive potential of PBR-HPBCD and PLA-HPBCD complex. (A) The number of implantation sites observed on Day 16 of Pregnancy (B) Number of litters born. Abbreviations are given in Table 1

Figure 3. Endocrinological evaluation of PBR-HPBCD at 250 mg/kg in OVX (Ovariectomized)(A) Estrogenic/anti-estrogenic activity (B) Progesterone/anti-progesterone activity

Figure 4. Representative 600 MHz NMR spectra of the serum obtained from mature female rats in pro-estrous phase (A) prior dosing, (B) post-treatment with the hydro-ethanolic extract of *P. betel* root and (C) the complexation product of the extract and HPBCD

Figure 5 (A-F). OPLS-DA plot of ^{1}H NMR spectral data of the serum collected prior and after xenobiotic administration (1 to 6 and 13 to 18=pre-treatment, 7 to 12 and 19 to 24=post-treatment of ethnomedicinal preparation and developed formulation, respectively). Panel (A) and (B) are the line and score plots, (C) and (E) are the contribution plots, and (D) and (F) are the scatter plots depicting the variations in metabolite profiling after the treatment of extract preparation and developed formulation, respectively.

Figure 6. Characterization of PLA-HPBCD nanoparticle (A) DLS (B) SEM (C) TEM (D) *in-vitro* release; The red line (top) shows the release of PLA from PLA-HPBCD complex while the black line (bottom) shows the release of solitary PLA without any complex.

Figure 7. PLA-HPBCD binding interactions *via* molecular docking. (A) Inclusion of PLA within HPBCD central cavity (B) Polar and hydrogen bonds between PLA and HPBCD. The colors are as per standard international conventions used to depict elements (hydrogen-grey, oxygen-red, nitrogen-blue, C-H bond-green)

Figure 8. Serum endocrinology and cytokine profile with PLA-HPBCD nanoconjugate (n=6). (A) Endocrinology; * denotes concentration in pg/mL and # denotes concentration in ng/mL. (B) serum interleukin profile. The observations are based on a group of six female Wistar rats (biological replicates, n=6), blood sample from each rat was also analyzed in three technical replicates. The values are represented as mean ± standard deviation.

Table 1 Assessment of contraceptive property

Table 2 Assessment of reversible contraceptive property and chronic toxicity

Table 1 Contraceptive property assessment

Group	Test substance	Oral dose (mg/kg)	n	nP	PI	nCL	nI	nL	nLD	mLW	VI(%)
C	Vehicle	-	6	6	-	9.3±0.2	8.7±0.2	8.3±0.2	0.0±0.0	15.4±0.1	100±0.0
T1	PBR-HPBCD	125	6	5	16.7	7.0±0.7*	4.0±0.9	3.4±0.4	1.6±0.5	15.7±0.5	48.0±19.1
T2	PBR-HPBCD	250	6	0	100	4.1±0.2	0.0±0.0	-	-	-	-
T3	PBR-HPBCD	400	6	0	100	3.3±0.2	0.0±0.0	-	-	-	-
T4	PBR-HPBCD	500	6	0	100	3.3±0.2	0.0±0.0	-	-	-	-
T5	PLA-HPBCD	2.5	6	2	60	5.2±0.4	1.5±0.5	1.0±0.0	1.0±0.0	-	0.0±0.0
T6	PLA-HPBCD	5	6	0	100	4.3±0.1	0.0±0.0	-	-	-	-
T7	PLA-HPBCD	10	6	0	100	3.8±0.2	0.0±0.0	-	-	-	-

n, nP, PI, nCL, nI, nL, nLD, mLW and VI represent the number of animals in a group, the number of pregnant animals, percentage pregnancy interception, the number of corpora lutea, the number of implantation sites, the number of litters born in aparturition, the number of litters that died within 7 days of parturition, mean live litter weight on day 7 and viability index, respectively. The results are expressed as mean ±S.E.M. The differences are significant relative to the control group (C) at $p<0.05$ except $*0.1>p>0.05$

Table 2 Reversible contraceptive property assessment and chronic toxicity studies

Parameter	Unit	Control (n=6)	Test (n=6)	% changes	Statistical parameters	
					ANOVA (F)	Significance (p)
Number of litter born	-	8.33±0.42	8.83±0.31	6.00	1.88	0.50
Viability index	-	100.0±0.0	100.00±0.00	0.00	-	-
Mean litter weight	g	14.97±0.15	15.06±0.17	0.57	1.29	0.79
SGPT	IU/L	26.42±0.77	28.28±1.00	7.04	1.70	0.57
SGOT	IU/L	21.37±0.71	21.49±0.39	0.56	3.24	0.22
ALP	IU/L	76.66±2.23	74.54±1.93	-2.76	3.09	0.24
Uric acid	mg/dL	6.13±0.19	6.29±0.12	2.61	2.61	0.32
Creatinine	mg/dL	0.31±0.01	0.31±0.00	-1.60	2.76	0.29
MDA	µg/mL	2.89±0.10	2.91±0.05	0.63	3.33	0.21
GSH	µg/mL	77.36±1.64	77.39±1.48	0.04	1.23	0.83
NO	µg/mL	0.58±0.02	0.58±0.01	-0.29	4.57	0.12

The results are presented as mean ± S.E.M.

SGPT- Serum Glumatate Pyruvate Transminase; SGOT- Serum Glumatate Oxaloacetate Transminase; ALP- Alkaline Phosphatase; MDA- Malondialdehyde; GSH- Reduce Glutathione; NO- Nitric Oxide

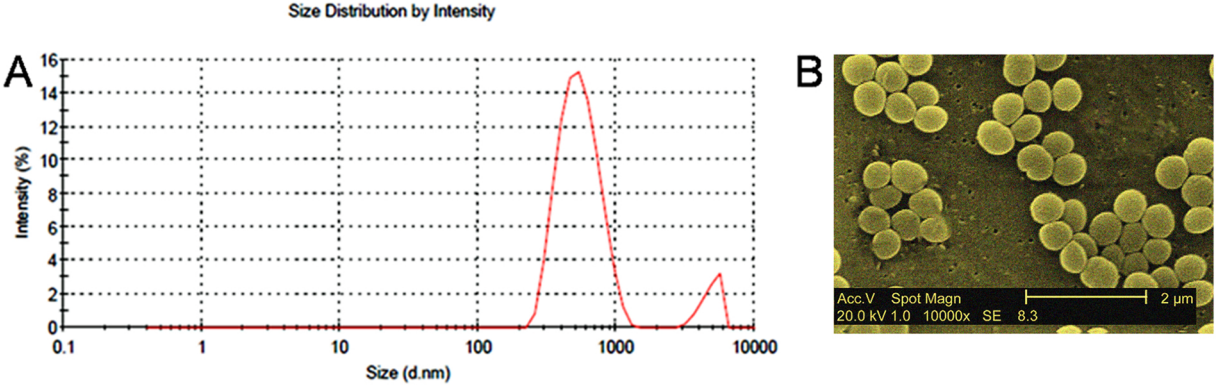
A
Size Distribution by Intensity
Intensity (%)
0
2
4
6
8
10
12
14
16
0.1
1
10
100
1000
10000
Size (d.nm)
B
Acc.V Spot Magn
2 µm
20.0 kV 1.0 10000x SE 8.3

Figure 1

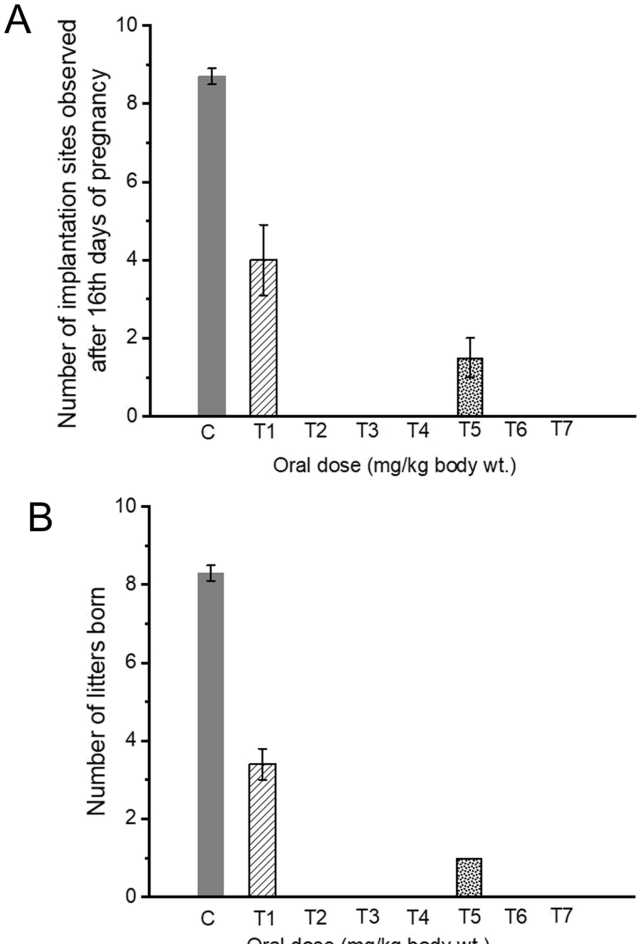
A
Number of implantation sites observed after 16th days of pregnancy
10
8
6
4
2
0
C
T1
T2
T3
T4
T5
T6
T7
Oral dose (mg/kg body wt.)
B
Number of litters born
10
8
6
4
2
0
C
T1
T2
T3
T4
T5
T6
T7
Oral dose (mg/kg body wt.)

Figure 2

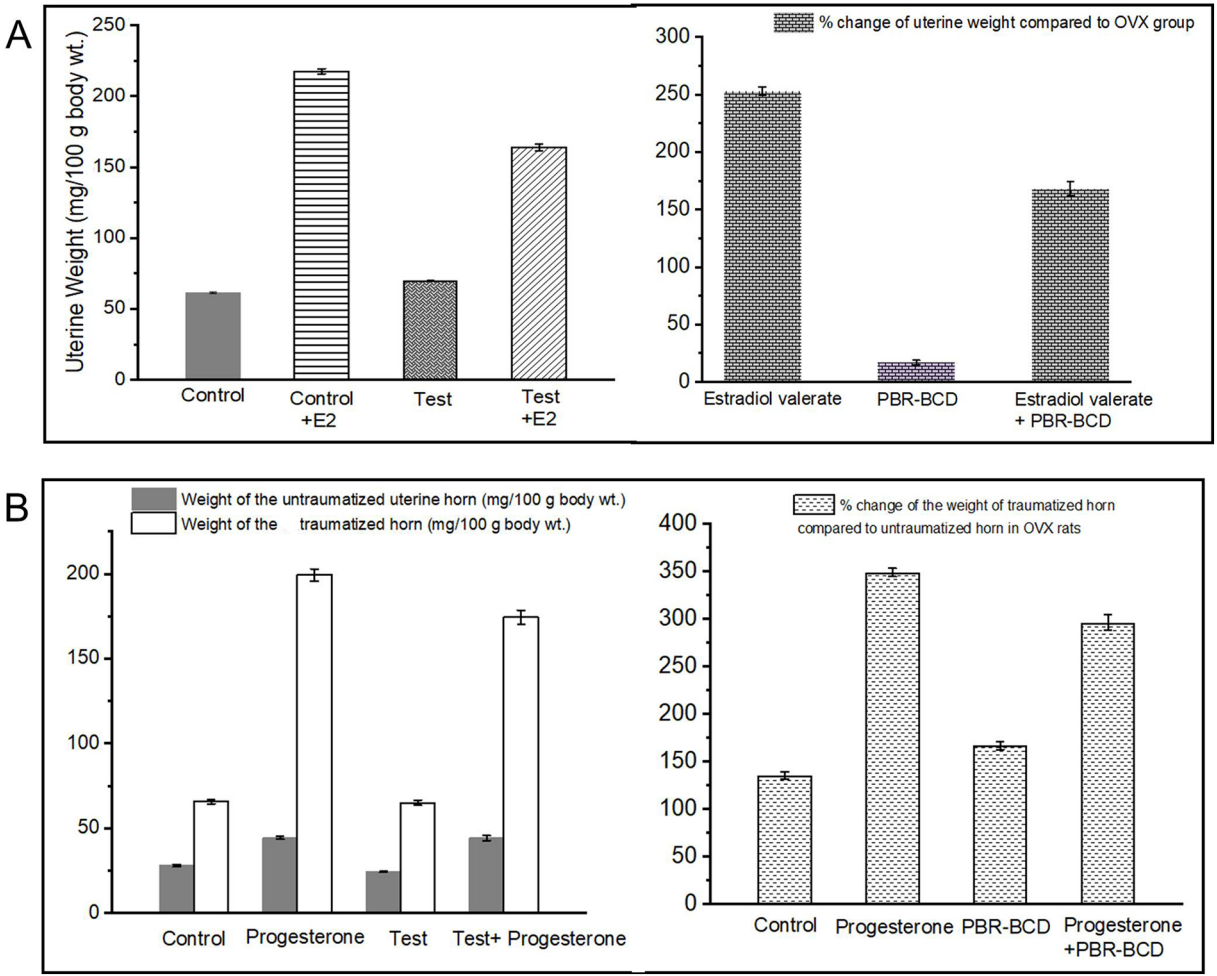
A
Uterine Weight (mg/100 g body wt.)
250
200
150
100
50
0
Control
Control +E2
Test
Test +E2
% change of uterine weight compared to OVX group
300
250
200
150
100
50
0
Estradiol valerate
PBR-BCD
Estradiol valerate + PBR-BCD
B
Weight of the untraumatized uterine horn (mg/100 g body wt.)
Weight of the traumatized horn (mg/100 g body wt.)
200
150
100
50
0
Control
Progesterone
Test
Test+ Progesterone
% change of the weight of traumatized horn compared to untraumatized horn in OVX rats
400
350
300
250
200
150
100
50
0
Control
Progesterone
PBR-BCD
Progesterone +PBR-BCD

Figure 3

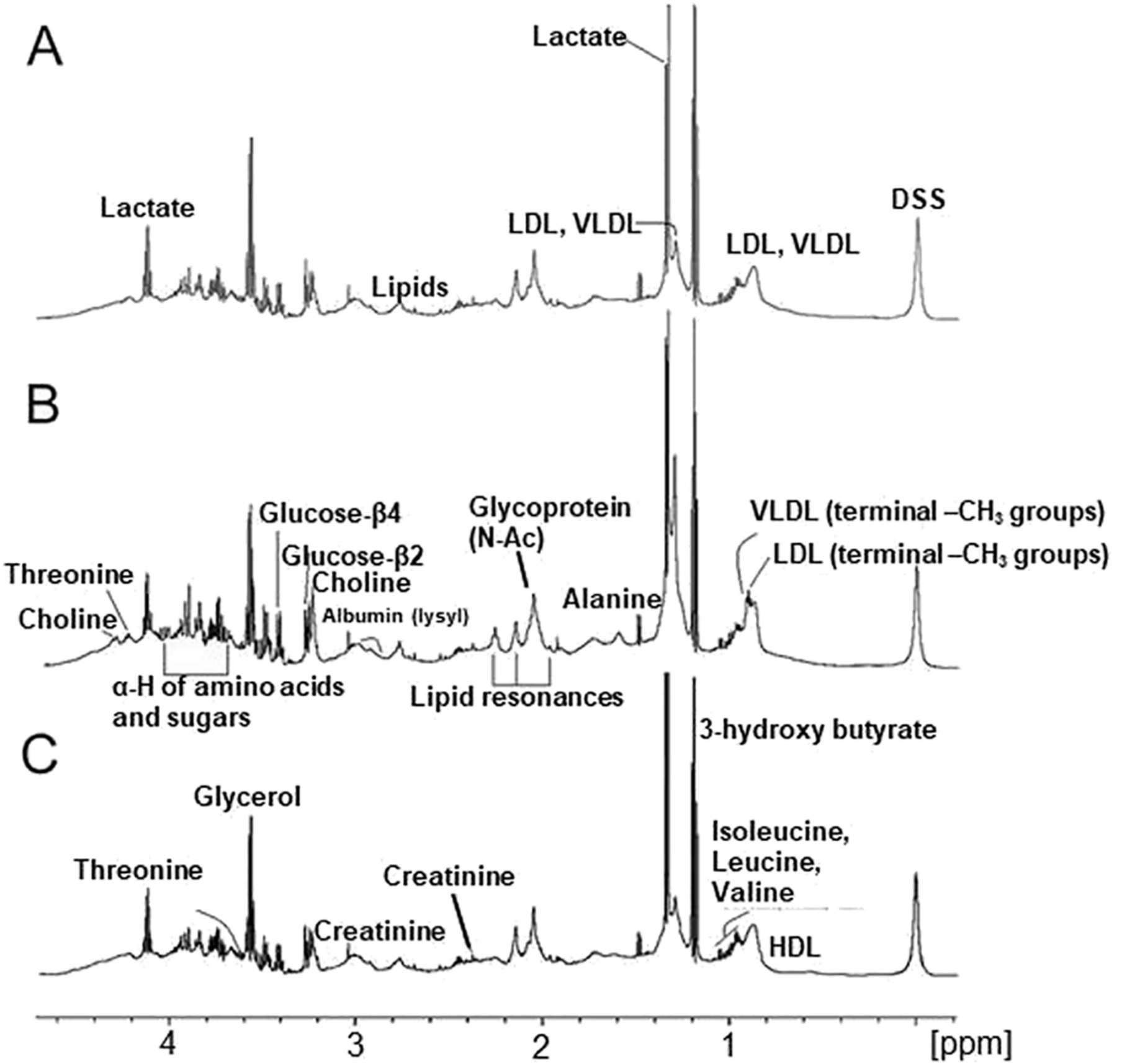
A
Lactate
Lactate
LDL, VLDL
LDL, VLDL
DSS
Lipids
B
Glucose-β4
Glycoprotein
(N-Ac)
VLDL (terminal –CH3 groups)
Glucose-β2
LDL (terminal –CH3 groups)
Threonine
Choline
Choline
Alanine
Albumin (lysyl)
α-H of amino acids
and sugars
Lipid resonances
3-hydroxy butyrate
C
Glycerol
Isoleucine,
Leucine,
Valine
Threonine
Creatinine
Creatinine
HDL
4
3
2
1
[ppm]

Figure 4

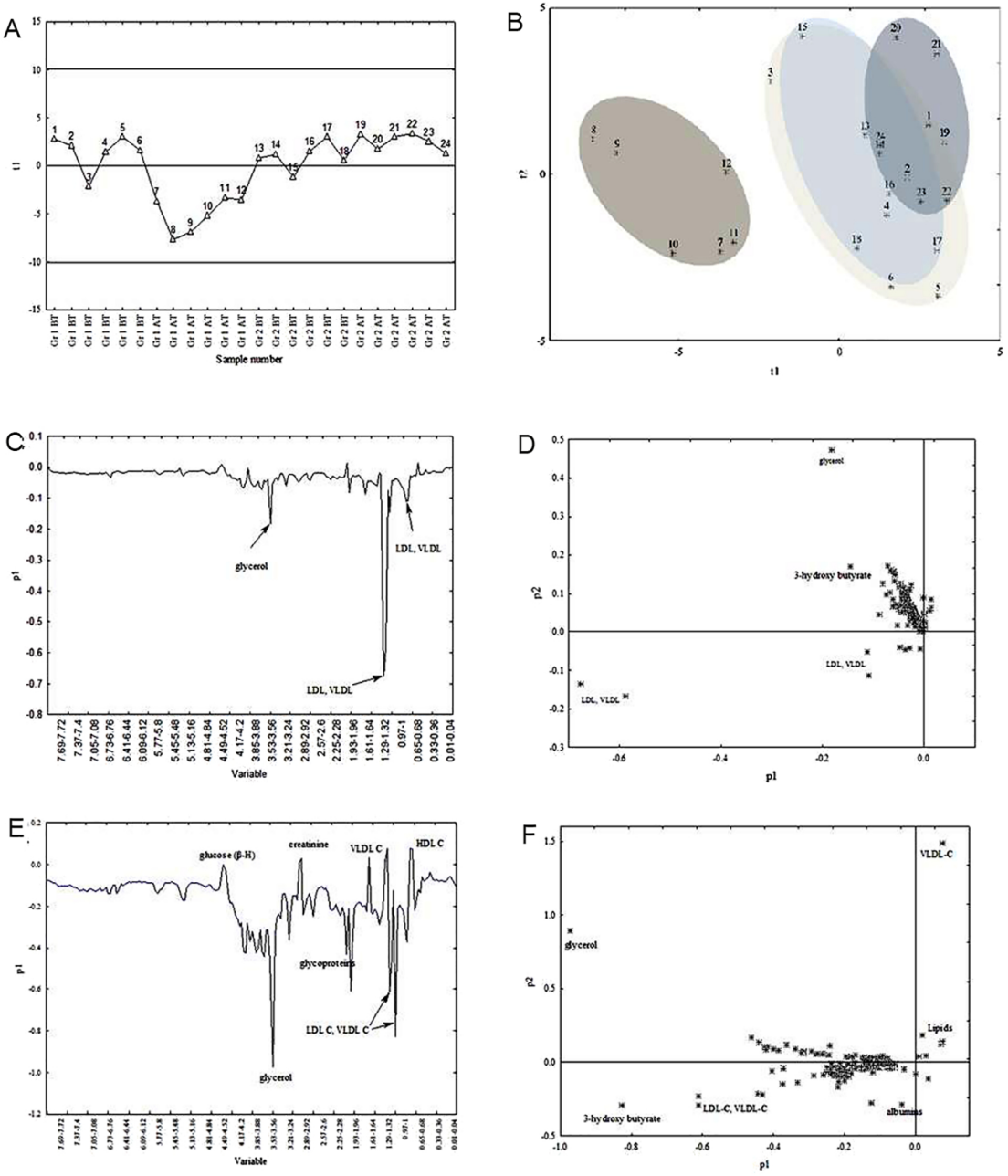
A
t1
Sample number
Gr1 BT
Gr1 AT
Gr2 BT
Gr2 AT
B
t1
t2
C
p1
glycerol
LDL, VLDL
Variable
D
p1
p2
glycerol
3-hydroxy butyrate
LDL, VLDL
E
p1
glucose (β-H)
creatinine
VLDL C
HDL C
glycoproteins
LDL C, VLDL C
glycerol
Variable
F
p1
p2
VLDL-C
glycerol
Lipids
3-hydroxy butyrate
LDL-C, VLDL-C
albumins

Figure 5

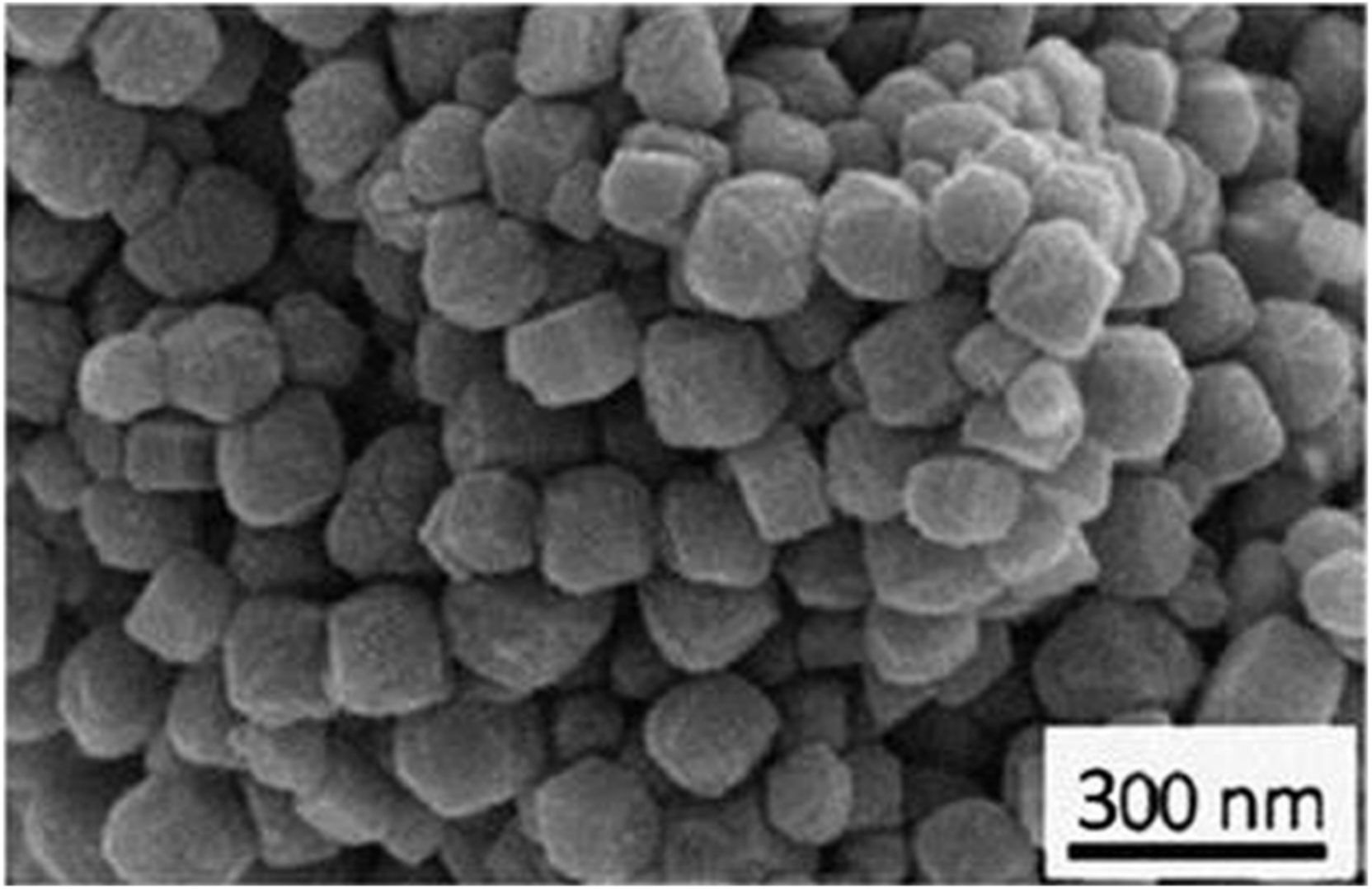

Figure 6

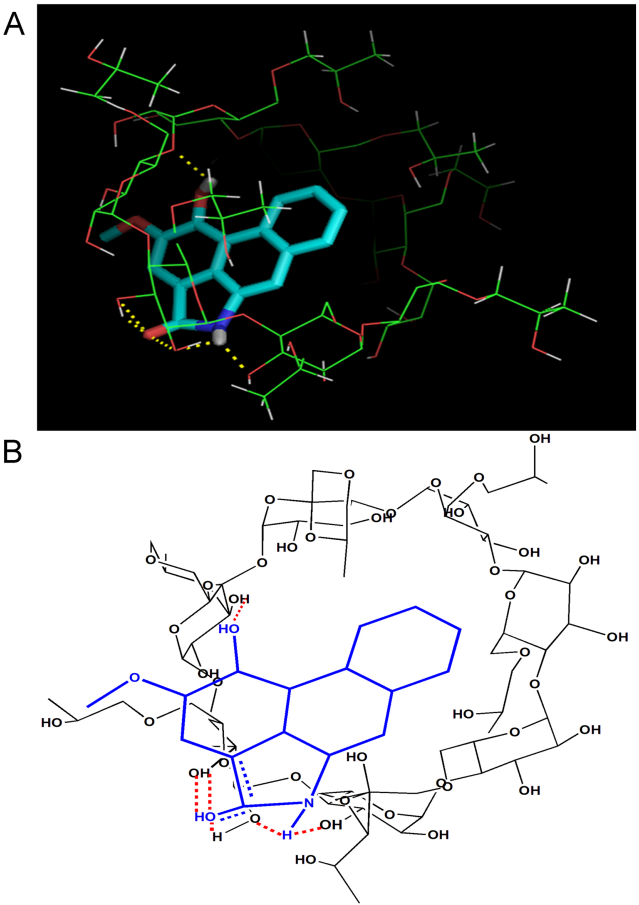

Figure 7

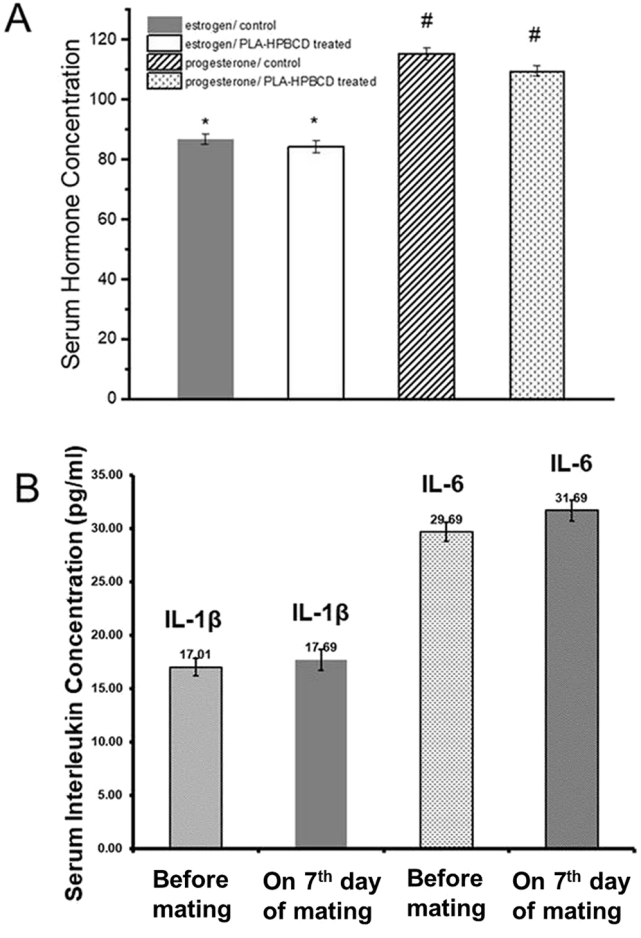
A
estrogen/ control
estrogen/ PLA-HPBCD treated
progesterone/ control
progesterone/ PLA-HPBCD treated
Serum Hormone Concentration
0
20
40
60
80
100
120
*
*
#
#
B
Serum Interleukin Concentration (pg/ml)
0.00
5.00
10.00
15.00
20.00
25.00
30.00
35.00
IL-1β
17.01
IL-1β
17.69
IL-6
29.69
IL-6
31.69
Before mating
On 7th day of mating
Before mating
On 7th day of mating

Figure 8